Microstructure and annealing behavior of a modified 9Cr-1Mo steel after dynamic plastic deformation to different strains

Zhang, Zhenbo; Mishin, Oleg; Tao, N.R.; Pantleon, Wolfgang

Published in:
Journal of Nuclear Materials

Link to article, DOI:
10.1016/j.jnucmat.2014.12.001

Publication date:
2015

Document Version
Peer reviewed version

Microstructure and annealing behavior of a modified 9Cr–1Mo steel after dynamic plastic deformation to different strains

Z.B. Zhang[1,4], O.V. Mishin[1,4], N.R. Tao[2,4], W. Pantleon[3,4]

[1]Danish-Chinese Center for Nanometals, Section for Materials Science and Advanced Characterization, Department of Wind Energy, Technical University of Denmark, Risø Campus, 4000 Roskilde, Denmark
[2]Shenyang National Laboratory for Materials Science,Institute of Metal Research, Chinese Academy of Science, Shenyang 110016, China
[3]Section for Materials and Surface Engineering, Department of Mechanical Engineering, Technical University of Denmark, 2800 Kgs.Lyngby, Denmark
[4]Sino-Danish Center for Education and Research

Abstract

The microstructure, hardness and tensile properties of a modified 9Cr–1Mo steel processed by dynamic plastic deformation (DPD) to different strains (0.5 and 2.3) have been investigated in the as-deformed and annealed conditions. It is found that significant structural refinement and a high level of strength can be achieved by DPD to a strain of 2.3, and that the microstructure at this strain contains a large fraction of high angle boundaries. Considerable structural coarsening of the deformed microstructure in the high-strain and low-strain samples,without pronounced recrystallization, was observed after annealing at for 1 h at 600 °C and 650 °C, respectively. Both coarsening and partial recrystallization took place in the high-strain sample during annealing at 650 °C for 1 h. The annealing treatments result in softening and a loss of strength. It is found that whereas coarsening alone is detrimental for strength with only a very little gain in ductility, coarsening combined with partial recrystallization enables a combination of significantly increased ductility and comparatively high strength.

Keywords: Ferritic/martensitic steel; Dynamic plastic deformation; Strength; Thermal stability

1. Introduction

Ferritic/martensitic steels containing 9 to 12 wt.%Cr are considered to be candidate structural materials for ultra-supercritical coal power plants and nuclear reactors because these steels are characterized by higher thermal conductivity, lower thermal expansion and better swelling resistance than the commonly used austenitic stainless steels [1–3]. It has been suggested that irradiation induced swelling can be reduced in materials with well-refined microstructures, and therefore such materials may exhibit improved irradiation tolerance compared to their coarse-grained counterparts [4–7]. One way to achieve grain refinement (and increase strength simultaneously) is via plastic deformation, when original grains become subdivided by dislocation boundaries. It has been shown that with increasing strain the boundary spacing decreases, whereas the average misorientation between subgrains becomes higher[8], which typically contributes to increased levels of strength. It is however known that microstructures refined by plastic deformation are often unstable at elevated temperatures. Therefore, the thermal stability of the microstructure and the changes in mechanical properties of such materials during thermal exposure are important aspects of their characterization.

In the present work, structural refinement in a modified 9Cr–1Mo steel is achieved via dynamic plastic deformation (DPD) [9]. DPD is utilized in this study because deformation at high strain rates has been previously shown to be more effective in subdividing the microstructure by dislocation boundaries than low-strain rate deformation [10–12]. The microstructure processed by DPD to different strains and its stability during subsequent annealing are investigated using transmission electron microscopy (TEM) and electron backscatter diffraction (EBSD). The study of the microstructural evolution is complimented by analysis of hardness and tensile test data. The results obtained in the present work are compared with the literature data for ECAE-processed ferritic/martensitic steels with similar compositions.

2. Experimental

A modified 9Cr–1Mo steel (X10CrMoVNb9–1) [12] was received in the form of a hot-extruded rod normalized at 1040 °C for 1.4 h, tempered at 770 °C for 5 h and finally stress-relieved at 740 °C. Cylindrical samples with a longitudinal direction (LD) parallel to the extrusion axis of the as-received rod, and with a size of 9 mm in diameter and 12 mm in height were machined for DPD. The samples were compressed at room temperature to different strainswithan initial strain rate of 10^2–10^3 s^{-1}. The compression axis (CA) was parallel to the LD. Samples compressed to an equivalent von Mises strain of either 0.5 or 2.3 were taken for further microstructural examinations before and after annealing for 1 h at 600 °C and 650 °C.

The microstructure of the as-received, deformed and annealed samples was investigated using both TEM and EBSD. The microstructure of each sample was inspected in the central part in a section that contained the LD. TEM thin foils were prepared by twin-jet electropolishing in a solution consisting of ethanol (70%), water (12%), 2-butoxy-ethanol (10%), and perchloric acid (8%). The foils were investigated in a JEOL 2000FX microscope operating at 200 kV.A Zeiss Supra 35 field emission gun scanning electron microscope equipped with a Channel 5 system from HKL Technology was used for the EBSD analysis.Step sizes of 20 nm and 100 nm were applied for EBSD measurements in the as-deformed and the annealed conditions, respectively. Because of the limited angular resolution of the EBSD technique [13,14], only misorientationsangles above 2° were considered when measuring the boundary spacing and fractions of different boundary types. Highangle boundaries (HABs) were defined as those with misorientations larger than 15°. Area fractions of the recrystallized regions in the annealed conditions were also determined from the EBSD data. Recrystallized grains were defined as regions with an equivalent circular diameter of at least 3 μm, predominantly surrounded by HABs and not containing misorientations above 2° in their interior [15].

Dog-bone shaped tensile test specimens with a gauge section of $5 \times 1 \times 0.5$ mm^3 were prepared from the sample deformed to a strain of 2.3, both in the as-deformed conditionand after subsequent annealing.Tensile tests were conducted using an Instron 5848 MicroTester at room temperature withan initial strain rate of 5×10^{-3} s^{-1}. A MTS LX300 laser extensometer was used for measuring engineering strain during the test.As the final diameter of the sample compressed to a strain of 0.5 was too small to machineappropriatetensile specimens, only Vickers hardness was measured in the center of this sample. All Vickers hardness measurements were performed by aStruersDuraScan fully automatic hardness tester, applying a load of 1 kg and a dwell time of 10 s.

3. Results

3.1 As-received material

The as-received microstructure mainly consists of tempered martensitic laths within prior austenitic grains. The prior austenite grain boundaries (PAGBs) and martensitic boundaries (MBs) are decorated by coarse $M_{23}C_6$ particles (see Fig.1), while much smaller MX type carbonitride particles are distributed randomly in the matrix. The sample contains a high dislocation density, which is typical of the tempered martensitic structure. The average subgrain size measured in TEM images in this as-received material is approximately 0.7 μm. The EBSD data indicate that the spacing between HABs (d_{HAB} in Table 1) is 2.4 μm, and the HAB fraction (f_{HAB}) is 46% [9].

3.2 Samples after DPD

The hardness of the DPD samples increases with increasing strain, as shown in Fig.2a. The increase in hardness is rapid for strains below 1, whereas for the higher strains the hardness changes very little. Based on the data in Fig.2a, two samples deformed to a strain of either 0.5 or 2.3, characterized by significant differences in hardness (see also Table 1), were selected for microstructural analysis.

After deformation to a strain of 0.5, the microstructure is subdivided by dislocation cell boundaries with an average boundary spacing of 190 nm(see Fig.3a), as measured along the CA. Since misorientations across these new cell boundaries are typically very low, the fraction of LABs increases,while the fraction of HABs decreases compared to those in the as-received condition (Table 1).At a strain of 2.3, the microstructure is well-refined by lamellar boundaries aligned almost perpendicular to the CA (see Fig.3b). Fig.4 provides evidence that the directionality of the lamellar boundaries can be disrupted around some coarse (>200 nm) particles (see Fig.4a), which results in the formation of so-called particle deformation zones. Such zones are not observed around smaller particles (see Fig.4b). The average spacing measured in the TEM images between the lamellar boundaries is 98 nm. As expected, the spacing $d_{\theta>2^\circ}$ for boundaries with misorientations above 2° measured inthe EBSD data is somewhat larger, 110 nm. The HAB spacing is 810 nm and 200 nm after strains of 0.5 and 2.3, respectively. The HAB fraction increases with increasing strain from 23% after a strain of 0.5 to 50% after a strain of 2.3 (Table 1).

3.3 Annealed samples

During annealing the DPD samples soften with a pronounced drop in hardness taking place for 550 °C and above in the sample deformed to a strain of 2.3 and for 600 °C and above in the sample deformed to a strain of 0.5 (see Fig.2b). In this low-strain sample, annealing leads to structural coarsening with no appreciable recrystallization even after 1 h at 650 °C (see Fig.5 and Table 1). The structural coarsening is accompanied by softening when the hardness decreases from 304 HV1 in the deformed material to 251 HV1 after 1 h at 650 °C (Table 1).

Annealing of the high-strain sample at 600 °C for 1 h also results in structural coarseningonly, during which the nanoscale lamellar structure produced by DPD is replaced by coarser and nearly equiaxedsubgrains (see Fig.6a and Fig.7a), and the hardness decreases from 365 HV1 to 273 HV1 (see Table 1). In contrast, when the high-strain material is annealed at 650 °C, both coarsening and pronounced partial recrystallization take place (see Fig.6b). The area fraction of recrystallized microstructure after 1 h at 650 °C is 12%, and the hardness is 228 HV1, i.e. lower than in the low-strain sample annealed at the same temperature (see Table 1). In each sample annealed either at 600 °C or

650 °C, the HAB spacing and the HAB fraction both increase significantly compared to those in the deformed samples (Table 1).

3.4 Tensile properties

Tensile properties were measured for the as-received condition and after DPD to a strain of 2.3 as these samples were large enough for preparing tensile test specimens in contrast to the sample compressed to a strain of 0.5 (see section 2). From the stress-strain curves in Fig.6 it is seen that the ultimate tensile strength (UTS) increases from 675 MPa in the as-received sample to 1247 MPa after DPD, while the total elongation to failure in the DPD-processed material becomes very small, 5%. Annealing at 600 °C for 1 h improves the total elongation only slightly, to ~7%, but the strength is reduced considerably, to 942 MPa. Only after annealing at 650 °C for 1 h a significant increase in the total elongation to ~11% is achieved, though it remains still lower than that in the as-received condition (see Table 1). The UTS after this annealing treatment is 811 MPa.

4. Discussion

4.1 Microstructure evolution

During DPD of the modified 9Cr–1Mo steel the initial microstructure containing tempered martensite evolves first into a typical dislocation cell structure at a strain of 0.5, and further to a nanoscale lamellar structure at a strain of 2.3. Morphologically, these structures are similar to that observed in nickel after compression by DPD [11,16]. It is considered that the high dislocation density, particles and finely spaced martensitic boundaries present in the initial microstructure impose significant effects on the microstructure evolution during additional deformation[17,18], contributing to the very fine boundary spacing observed after DPD.

The results obtained in our work can be compared with those on the modified 9Cr–1Mo steel cold deformed by equal channel angular extrusion(ECAE) [19,20]. Similar to our observations for the low-strain DPD sample, the initial tempered martensitic structure observed in [19] evolved into a nearly equiaxedsubgrain structure already after a single pass through an ECAE die with 90° angle between channels (strain ~1.15). The deformation by ECAE appeared, however, to be less effective for structural refinement than DPD as the average subgrain size was found to be 0.4 μm after a strain of 1.15 and 0.2–0.3 μm and for strains of 3.8–4.6 [19,20] (note that a strain of 3.8 corresponds to 6 passes through a 120° die in [19]). Thus, the subgrain size after a rather high strain by ECAE was similar to that obtained in our material processed by DPD to a strain of only 0.5. The more rapid refinement observed in our experiment compared to that by ECAE can be attributed to the higher strain rates during DPD, which generates a higher density of dislocations forming finely spaced dislocation boundaries [10–12].

The high energy stored in the form of dislocations and deformation-induced boundaries makes the DPD microstructure unstable at elevated temperatures. As the driving force for coarsening and recrystallization increases with increasing strain, i.e. with decreasing boundary spacing, more pronounced microstructural changes during annealing and more significant softening are observed in the high-strain sample than in the low-strain sample. Although the high stored energy makes the deformed microstructure rather unstable during annealing, small carbide particles present in it hinder very rapid recrystallization by pinning some migrating boundaries, as is evident from Fig.7b, where cusped grain boundaries are observed in the vicinity of particles.

4.2 Evolution of mechanical properties

Structural refinement by DPD makes the modified 9Cr–1Mo steel harder and significantly increases its strength. After DPD to a strain of 2.3 the hardness increased from 205 HV1 to 365 HV1 and the UTS was almost doubled (from 675 MPa to 1247 MPa). These values after DPD are much greater than those in the ECAE-processed 9Cr–1Mo steel, where the hardness was only 320 HV0.1 even a strain of 4.6 [20]. Fan et al. [19] reported that the UTS after a strain of 2.5 was 1004 MPa, i.e. ~20% lower than the strength of our DPD sample deformed to a similar strain. The UTS of our strain 2.3 DPD sample was higher than that obtained during low strain rate deformation even after a strain of 3.8 by ECAE [19], which reflects the difference in the extent of structural refinement between the two deformation techniques, i.e. the finer boundary spacing after DPD compared to that after ECAE.

The significant strengthening of the modified 9Cr–1Mo steel by DPD is accompanied by a dramatic reduction in ductility, where the total elongation is only 5% after a strain of 2.3. The lack of ductility is typical for many heavily cold-deformed materials demonstrating very limited work-hardening[21–23]. Deformation at elevated temperatures or post-deformation heat-treatments can improve ductility (which can be important for further forming operations), but the strength in this case is not as high as in cold-deformed samples with no additional annealing [20]. In our material, annealing at 600°C for 1 h of the sample deformed to a strain of 2.3 leads to softening and a considerable loss of strength with a very minor increase in elongation (Fig.8), which indicates that the coarsening of the deformed microstructure alone is detrimental for strength with only a very little gain in ductility. In contrast, coarsening combined with partial recrystallization enable significantly increased ductility andstill comparatively high strength (see Fig.8 and Table 1).

5. Conclusions

1. The microstructure in the 9Cr–1Mo steel can be effectively refined by DPD. The boundary spacing measured along the compression axis decreases from 190 nm at a strain 0.5 to 98 nm at a strain of 2.3. At this large strain the HAB fraction in the deformed microstructure is 44%, as determined by EBSD. The structural refinement results in substantial strengthening of the material: the ultimate tensile strength increases from 675 MPa in the as-received condition to 1247 MPa after DPD to a strain of 2.3.

2. The high stored energy of the DPD samples affects the thermal stability of the deformed microstructure. The evolution of the microstructure in the high-strain sample annealed at 600°C for 1 h and in the low-strain sample annealed at 650°C for 1 h can be described as structural coarsening without pronounced recrystallization. Both coarsening and pronounced partial recrystallization are observed in the high-strain sample annealed at 650°C for 1 h.

3. The changes in the microstructure taking place during annealing result in a significant loss of strength. Whereas coarsening of the deformed microstructure alone is detrimental for strength and only very little affects the ductility, coarsening combined with partial recrystallization results in a combination of increased ductility and comparatively high strength.

Acknowledgements

The financial support from the Sino-Danish Center for Education and Research is gratefully acknowledged. ZBZ and OVM also gratefully acknowledge the support from the Danish National

Research Foundation (Grant No. DNRF86-5) and the National Natural Science Foundation of China (Grant No. 51261130091) to the Danish-Chinese Center for Nanometals.

References

[1] R.L. Klueh, K. Ehrlich, F. Abe, J. Nucl. Mater. 191 (1992) 116-124.
[2] R. Viswanathan, W. Bakker, J. Mater. Eng. Perform. 10 (2001) 81-95.
[3] R.L. Klueh, Int. Mater. Rev. 50 (2005) 287-310.
[4] B.N. Singh, Philos. Mag. 29 (1974) 25-42.
[5] M. Rose, A.G. Balogh, H. Hahn, Nucl. Instrum. Meth. B 127/128 (1997) 119-122.
[6] Y. Chimi, A. Iwase, N. Ishikawa, M. Kobiyama, T. Inami, S. Okuda, J. Nucl. Mater. 297 (2001) 355-357.
[7] C. Sun, K.Y. Yu, J.H. Lee, Y. Liu, H. Wang, L. Shao, S.A. Maloy, K.T. Hartwig, X. Zhang, J. Nucl. Mater. 420 (2012) 235-240.
[8] N. Hansen, D. Juul Jensen, Mater. Sci. Technol. 27 (2011) 1229-1240.
[9] Y.S. Li, N.R. Tao, K. Lu, Acta Mater. 56 (2008) 230-241.
[10] F. Huang, N.R. Tao, K. Lu, J. Mater. Sci. Techn. 27 (2011) 628-632.
[11] Z.P. Luo, O.V. Mishin, Y.B. Zhang, H.W. Zhang, K. Lu, Scr. Mater. 66 (2012) 335-338.
[12] Z.B. Zhang, O.V. Mishin, N.R. Tao, W. Pantleon, Mater. Sci. Technol. (2015) DOI: 10.1179/1743284714Y.0000000652.
[13] F.J. Humphreys, J. Mater. Sci. 36 (2001) 3833-3854.
[14] O.V. Mishin, L. Östensson, A. Godfrey, Metall. Mater. Trans. A 37 (2006) 489-496.
[15] G.L. Wu, D.J. Jensen, Mater. Character. 59 (2008) 794-800.
[16] Z.P. Luo, H.W. Zhang, N. Hansen, K. Lu, Acta Mater. 60 (2012) 1322-1333.
[17] R. Ueji, N. Tsuji, Y. Minamino, Y. Koizumi, Acta Mater. 50 (2002) 4177-4189.
[18] X. Huang, S. Morito, N. Hansen, T. Maki, Metall. Mater. Trans. A 43A (2012) 3517-3531.
[19] Z.Q. Fan, T. Hao, S.X. Zhao, G.N. Luo, C.S. Liu, Q.F. Fang, J. Nucl. Mater. 434 (2013) 417-421.
[20] T. Hao, Z.Q. Fan, S.X. Zhao, G.N. Luo, C.S. Liu, Q.F. Fang, Mater. Sci. Eng. A 596 (2014) 244-249.
[21] M. Song, R. Zhu, D.C. Foley, C. Sun, Y. Chen, K.T. Hartwig, X. Zhang, J. Mater. Sci. 48 (2013) 7360-7373.
[22] R. Song, D. Ponge, D. Raabe, J.G. Speer, D.K. Matlock,Mater. Sci. Eng. A 441 (2006) 1-17.
[23] Y.B.Zhang, O.V.Mishin, N.Kamikawa, A.Godfrey, W.Liu, Q.Liu, Mater. Sci. Eng. A 576 (2013) 160-166.

Table 1. Microstructural parameters (where d, $d_{\theta>2^\circ}$andd_{HAB} are spacings between different types of boundaries,f_{rex} is the recrystallized fraction andf_{HAB} is the HAB fraction)andmechanical propertiesof the 9Cr−1Mo steel after DPD and subsequent annealing.

Condition	TEM	EBSD				HV1	UTS (MPa)	Total elongation (%)
	d (nm)	$d_{\theta>2^\circ}$ (nm)	d_{HAB} (nm)	f_{rex} (%)	f_{HAB} (%)			
As-received	690	1110	2430	-	46	205±2	675±6	21.5±1.5

DPD 0.5	190	210	810	-	23	304±5	-	
DPD 2.3	98	110	200	-	50	365±3	1247±16	5.0±0.3
DPD 0.5 + 650°C 1 h	-	420	1240	1	32	251±6	-	
DPD 2.3 + 600°C 1 h		270	445	0	52	273±6	942±11	6.8±0.5
DPD 2.3 + 650°C 1 h	-	470	760	12	55	228±9	811±15	10.9±0.4

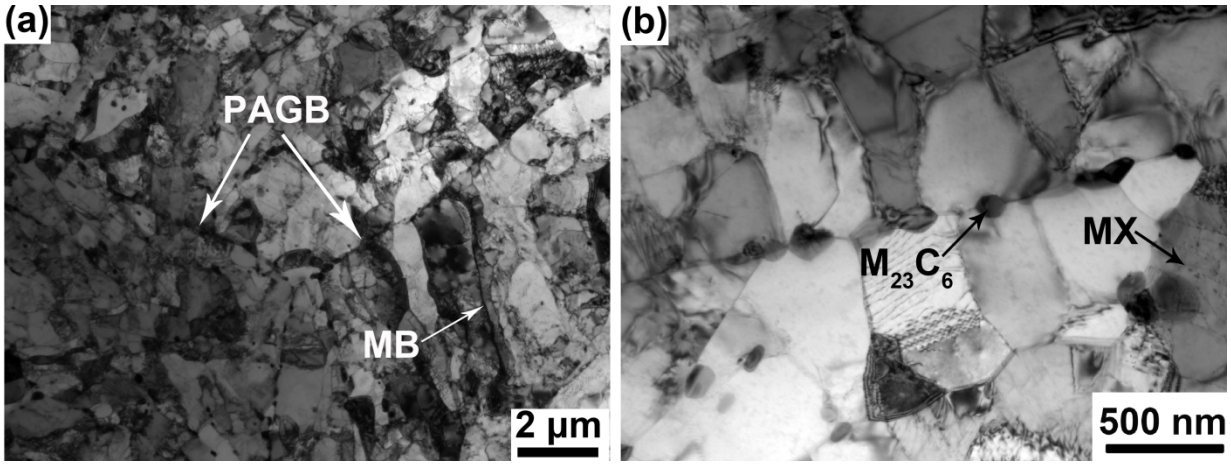

Fig.1 TEM images of the 9Cr–1Mo steel in the as-received condition: (a) an overview image showing the tempered martensite with prior austenite grain boundaries (PAGB) and martensitic boundaries (MB) indicated by arrows; (b) $M_{23}C_6$ carbides and MX type carbonitride particles present in the microstructure.

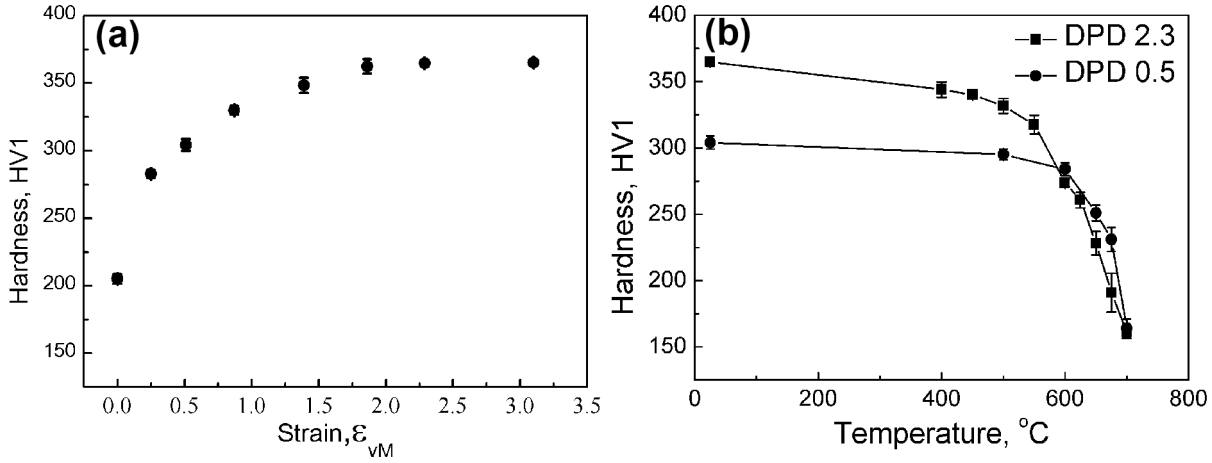

Fig.2 The evolution of Vickers hardness of the 9Cr–1Mo steel: (a) during DPD to different strains; (b) during annealing of two samples deformed to strains of 0.5 and 2.3

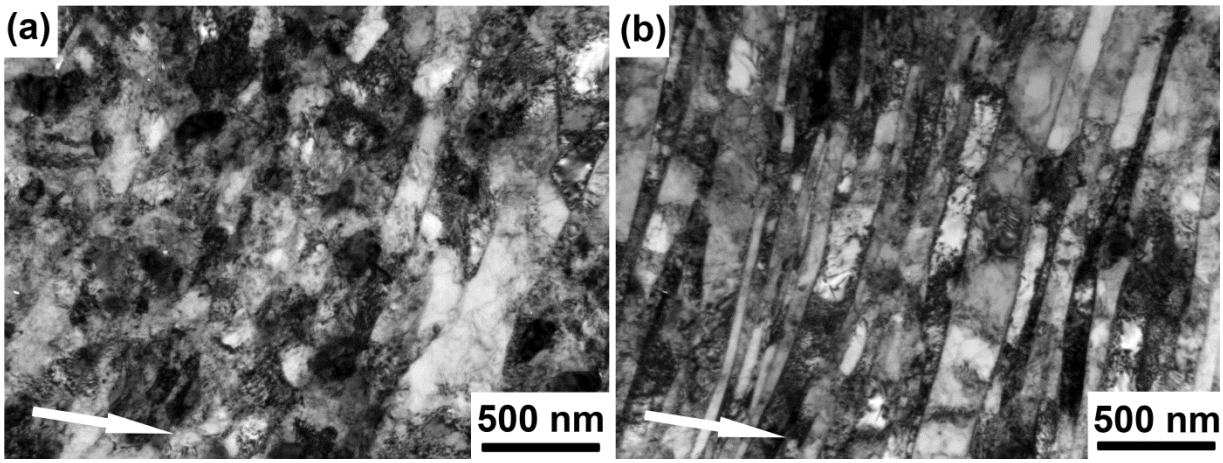

Fig.3 TEM images of the 9Cr–1Mo steel after DPD to a strain of (a)0.5 and(b)2.3. The compression axis is indicated by arrows.

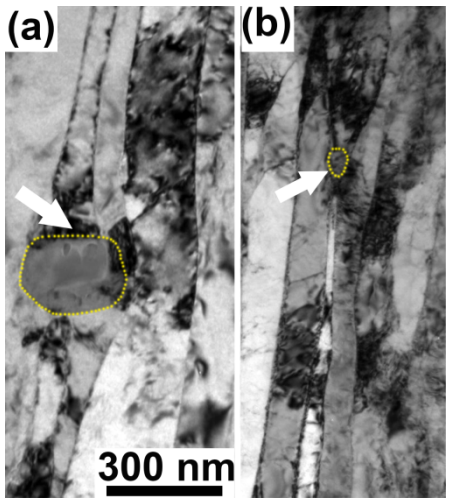

Fig.4 Microstructure in the vicinity of (a) coarse and (b)small particles marked by dashed linesand arrows.

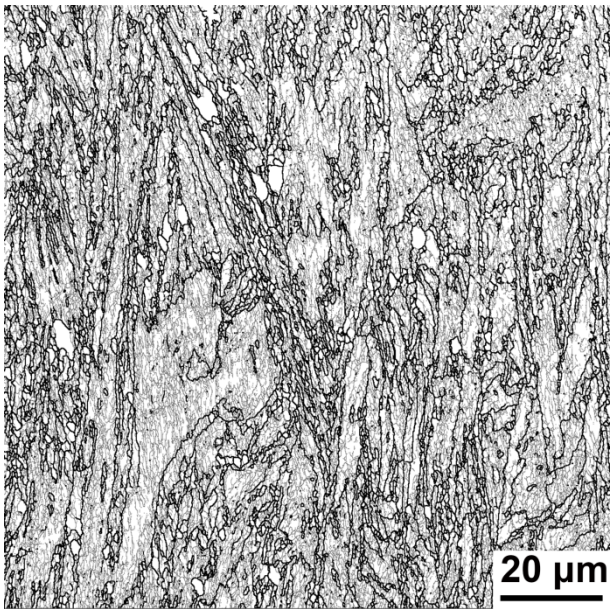

Fig.5 A boundary map obtained by EBSD of the 9Cr–1Mo steel deformed by DPD to a strain of 0.5 and subsequently annealed at 650 °C for 1 h. HABs and LABs are shown as black and gray lines, respectively. Recrystallized grains are seen in these maps as large white regions. The compression axis is parallel to the scale bar.

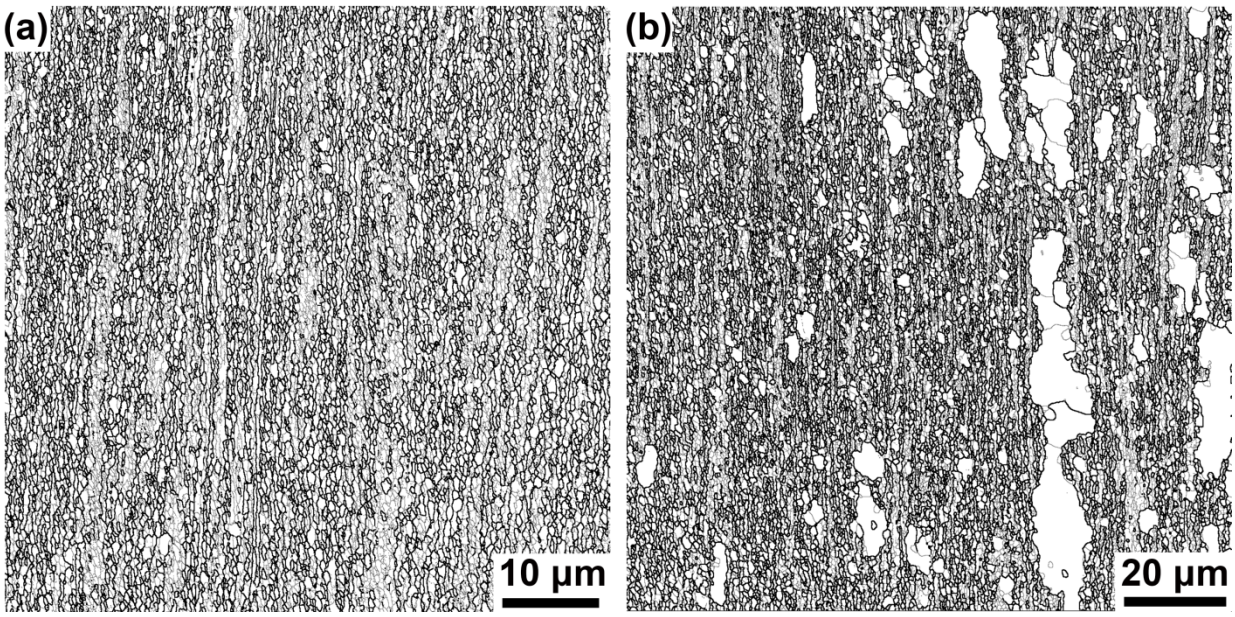

Fig.6 Boundary maps obtained by EBSD of the 9Cr–1Mo steel deformed by DPD to a strain of 2.3 and subsequently annealed at (a) 600 °C and (b) 650 °C for 1 h. HABs and LABs are shown as black and gray lines, respectively. Recrystallized grains are seen in these maps as large white regions. The compression axis is parallel to the scale bar.

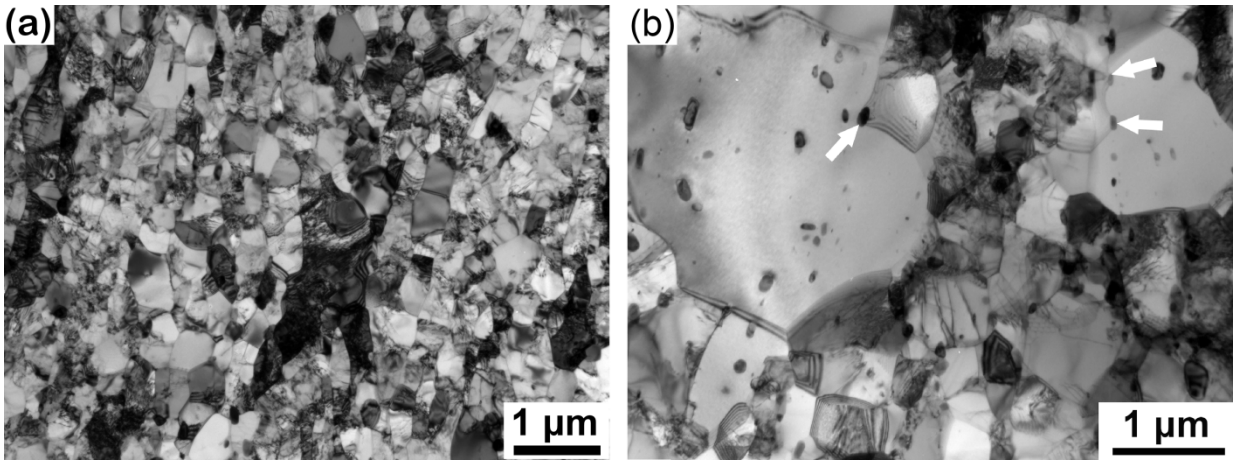

Fig.7 TEM images of the 9Cr–1Mo steel deformed by DPD to a strain of 2.3 and annealed at (a)600 °C and (b) 650 °C for 1 h. The arrows in (b) indicate cusped boundaries at particles.

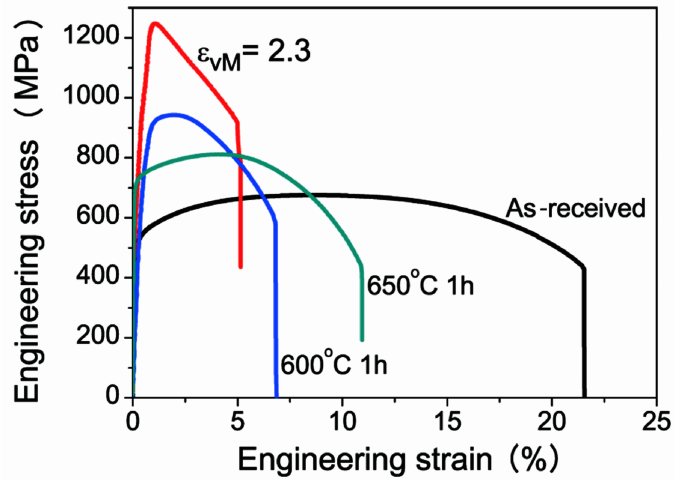

Fig.8 Stress-strain curves for the 9Cr–1Mo steel in the as-received condition and after DPD to a strain of 2.3 in the deformed and annealed conditions.